Ultrafast optical processes in nitrides

2001 J. Phys.: Condens. Matter 13 7075

(http://iopscience.iop.org/0953-8984/13/32/313)

INSTITUTE OF PHYSICS PUBLISHING JOURNAL OF PHYSICS: CONDENSED MATTER

J. Phys.: Condens. Matter **13** (2001) 7075–7087 PII: S0953-8984(01)24821-8

Ultrafast optical processes in nitrides

G Malpuech and A Kavokin

LASMEA–CNRS, Université Blaise Pascal, 24 avenue des Landais, 63177 Aubiere, France

Received 14 May 2001
Published 26 July 2001
Online at stacks.iop.org/JPhysCM/13/7075

Abstract

We discuss here so-called 'propagation phenomena' in nitrides, i.e. the phenomena of light–matter coupling at the femtosecond and picosecond time-scales. Specifics of nitrides, namely, giant oscillator strengths of A and B excitons and extremely important potential disorder in GaN and related structures makes the elastic scattering of light by excitons a dominant process that has a huge influence on all kinds of coherent optical spectrum. We show how to extract the oscillator strength and inhomogeneous broadening from the reflection and resonant Rayleigh scattering spectra of GaN-based QWs. Finally, we discuss the stability of excitonic complexes like charged trions in nitrides and the effect of the free electron–hole plasma on their optical properties.

1. Introduction

The exciton binding energy in GaN is about 25 meV [1], which corresponds exactly to the thermal activation energy k_bT at room temperature. Moreover, the exciton stability is considerably enhanced in quantum structures, which generally form the elementary cells of the new generations of light emitting devices. That is why the excitons are expected to play a major role in optical properties of nitride-based quantum structures even at room temperature. The excitons are only active in optics if coupled to light. This coupling results in exciton polaritons [2, 3], quasiparticles combining properties of photons and excitons. The ultrafast optical response of quantum structures is governed by the dynamics of the exciton polaritons. Their group velocity, ranging from almost zero to the light velocity in the media, will be a characteristic of the information transfer rate in future optical processors, thus it has a key importance for quite intriguing applications. Though the theory of exciton polaritons in bulk semiconductors was built almost 40 years ago by Hopfield and Agranovich [2], to calculate the polariton propagation in nitrides one should revise all existing theories. The huge additional complication comes from the potential disorder that is extremely strong even in high quality nitride-based heterostructures. The disorder comes from the random polarization fields, alloy and interface fluctuations, dislocations and impurities. Due to a potential disorder the number of discrete localized exciton states coupled to light amounts to a few million in a standard optical experiment. To describe the polariton propagation

in such a complicated system important approximations have to be adapted. The first of them is to *ignore* the microscopic parameters of each individual localized exciton state and to operate with macroscopic characteristics. These characteristics are the exciton radiative decay rate Γ_r, the value of the polarization field, the average distance d between the exciton localization centres, the average size r_{QD} of these localization centres and the broadening Δ of the frequency distribution of the exciton resonance. Any model operating with these macroscopic parameters is a phenomenological model. We would like to formulate and apply here a phenomenological model that takes into account the two most important effects that dominate the light–matter interaction in the system, namely, the exciton-polariton effect and the disorder scattering effect.

In this article, we present experimental and theoretical tools for the study of exciton properties versus disorder in nitride-based quantum structures. We show that resonant Rayleigh scattering (RRS) [4, 5] combined with conventional reflectivity measurements can easily allow determination of the most essential parameters of quantum well (QW) excitons if they are interpreted in the framework of an advanced Fourier spectroscopy analysis [6].

The RRS of light by quantum wells excitons is due to the breakdown by the disorder of the translation invariance in the plane of the QWs. In other words the disorder potential induces the localization of excitons in certain 'quantum-dot-like' states, and these localized excitons coherently scatter the light in all directions. The time-resolved RRS spectra are a direct probe of the statistical properties of the disorder [5]. The low intensity of the light scattered in a given direction makes the RRS experiment quite non-trivial to perform. In nitrides this problem is less important than in arsenides because of the strong disorder. Basically, scattering experiments are certainly the best adapted tool to study the exciton properties in nitride-based QWs. Time-resolved reflection measurements have equally been extensively used in conventional III–V semiconductors in order to determine the exciton properties [7]. In general, coherent time-resolved techniques have been found to be much more precise than the conventional cw reflectivity or transmission. However, the intensity of the time-resolved signal is proportional to $(\Gamma_r/\Delta)^2$ whereas the decay is roughly given by $1/\Delta$. The two last quantities are extremely small in most GaN/AlGaN QWs and the direct measurement of the time-resolved reflection remains a challenge from the experimental point of view. An indirect alternative way can be to perform the numerical Fourier transform of the cw experimental signals. Such a kind of treatment, currently performed in other fields of physics [8], has already successfully been applied on InGaAs QWs [9, 10]. It allows us to get signals extremely close to the real time resolved reflectivity and is potentially promising to extract the exciton oscillator strength and inhomogeneous broadening.

This paper is organized as follows. In the second part we present a new theory describing all types of coherent optical experiment (reflection, transmission, scattering) of confined localized excitons in the framework of a unified formalism. The model properly takes into account the renormalization effects associated with the exciton–light coupling as well as the structural disorder effects. In the third part we analyse theoretical RRS spectra of QWs and show how to extract from these spectra the information on excitonic statistics. We demonstrate that all the key parameters of the QW excitons can be obtained by performing angle- and time-resolved RRS experiments. The fourth part is devoted to the application of our formalism to analyse the experimental reflection spectra of GaN/AlGaN QWs. The numerical Fourier transform of steady-state reflection spectra of MBE grown GaN/AlGaN QWs is performed. This has allowed us to obtain the exciton oscillator strength and inhomogeneous broadening as a function of the QW width. A rapid decrease of the oscillator strength with the QW width increase has been found to be a consequence of the

exciton deformation by the polarization fields. This tendency is confirmed by a self-consistent variational calculation.

2. Formalism

Our formalism (see also [6]) is based on the Green-function approach to the problem of light–exciton coupling in low-dimensional structures [11] and the generalized scattering state technique for the light-pulse propagation in multilayer systems [4–12]. We consider each QW as an irregular array of quantum dots (QDs). The QDs represent shallow potential islands that weakly localize exciton wave-functions, so that the exciton wave-functions attributed to the neighbouring QDs may overlap. Each QD is characterized by a given exciton resonance frequency ω_n, and radius-vector $\vec{R}_n$ that denotes the centre of the localized exciton wave-function in the dot. We assume ω_n to be distributed with a function

$$f(\omega_1) = \frac{1}{\sqrt{\pi}\Delta} \exp\left[-\left(\frac{\omega_1 - \omega_0}{\Delta} \right)^2 \right] \tag{1}$$

where Δ describes the exciton inhomogeneous broadening.

Neglecting the deviations in the shape of the exciton wave-function localized in different dots, we solve the Maxwell equation:

$$\nabla \times \nabla \times \vec{E} = k_0^2 \vec{D} \tag{2}$$

where

$$\vec{D} = \varepsilon_b \vec{E} + 4\pi \vec{P}_{exc} \tag{3}$$

and

$$4\pi \vec{P}_{exc} = \sum_{n=1}^{N} T_n \Phi(\vec{r} - \vec{R}_n) \int \vec{E}(\vec{r}\,') \Phi(\vec{r}\,' - \vec{R}_n)\, \mathrm{d}\vec{r}\,' \tag{4}$$

with

$$T_n = \frac{\varepsilon_b \omega_{LT} \pi a_B^3}{\omega_n - \omega - \mathrm{i}\gamma}$$

k_0 being the wave-vector of the incident light in the media, ω_{LT} being the longitudinal–transverse splitting, ε_b being the background dielectric constant, a_B being the Bohr radius of the exciton in the bulk, γ being the homogeneous broadening and $\Phi(\vec{r})$ being the localized exciton wave-function taken with equal electron and hole co-ordinates. Further we assume equal shapes of $\Phi(\vec{r})$ for all QDs. Solving equation (2) we represent an electric field as

$$\vec{E}(\omega, \vec{r}) = \vec{E}_0 \exp(\mathrm{i}\vec{k}\vec{r}) + k_0^2 \sum_{n=1}^{N} T_n \int \mathrm{d}\vec{r}\,' \Phi(\vec{r}\,' - \vec{R}_n) G_0(\vec{r} - \vec{r}\,') \int \vec{E}(\vec{r}\,'') \Phi(\vec{r}\,'' - \vec{R}_n)\, \mathrm{d}\vec{r}\,'' \tag{5}$$

where $G_0(\vec{r} - \vec{r}\,') = \mathrm{e}^{\mathrm{i}k|\vec{r} - \vec{r}\,'|}/4\pi|\vec{r} - \vec{r}\,'|$ is the Green function for a zero-dimensional system and $\vec{k} = \vec{k}_0\sqrt{\varepsilon_b}$, is the wave-vector of the incident light in the media. It is convenient to multiply left and right parts of equation (5) by $\Phi(\vec{r} - \vec{R}_m)$ and integrate over $\vec{r}$. This procedure yields an expression for

$$\Lambda_m \equiv \int \vec{E}(\vec{r}) \Phi(\vec{r} - \vec{R}_m)\, \mathrm{d}\vec{r} = \int \vec{E}_0 \exp(\mathrm{i}\vec{k}\vec{r}) \Phi_{QD}(\vec{r} - \vec{R}_m)\, \mathrm{d}\vec{r} + \sum_{n \neq m}^{N} \Theta_{nm} \Lambda_n (1 - \Theta_{mm})^{-1} \tag{6}$$

where

$$\Theta_{nm} = k_0^2 T_n \int\int G_0(\vec{r} - \vec{r}')\Phi_{QD}(\vec{r}' - \vec{R}_n)\Phi_{QD}(\vec{r} - \vec{R}_m)\,\mathrm{d}\vec{r}'\,\mathrm{d}\vec{r}. \tag{7}$$

In the normal incidence case, the solution of equation (6) can be approximated by

$$\Lambda_m = \int \vec{E}_0\,\mathrm{e}^{\mathrm{i}\vec{k}\vec{r}}\Phi(\vec{r})\,\mathrm{d}\vec{r}\left(1 - \sum_{n=1}^{N}\Theta_{nm}\right)^{-1} \tag{8}$$

that allows us to express the electric field as

$$\vec{E}(\omega,\vec{r}) = \vec{E}_0\exp(\mathrm{i}\vec{k}\vec{r}) + k_0^2\sum_{n=1}^{N} T_n\int \mathrm{d}\vec{r}'\Phi(\vec{r}' - \vec{R}_n)G_0(\vec{r} - \vec{r}')$$
$$\times\int \vec{E}_0\,\mathrm{e}^{\mathrm{i}\vec{k}\vec{r}}\Phi(\vec{r})\,\mathrm{d}\vec{r}\left(1 - \sum_{m=1}^{N}\Theta_{nm}\right)^{-1}. \tag{9}$$

The Fourier transform of the electric field (9) yields its directional dependence which can be represented in the form

$$\vec{E}_d(\omega,\vec{k}_s) = \vec{E}_0\delta_{\vec{k},\vec{k}_s} + \vec{E}_0\sum_{m=1}^{N}\frac{\mathrm{i}\Gamma_0^{QD}}{\omega_m - \omega - \mathrm{i}\gamma}\left(1 - \sum_{n=1}^{N}\Theta_{nm}\right)^{-1}\exp(\mathrm{i}\vec{k}_s\vec{R}_m) \tag{10}$$

where

$$\Gamma_0^{QD} = \frac{1}{6}\omega_{LT}k_0^3 a_B^3\left(\int \mathrm{d}\vec{r}\cos(\vec{k}\vec{r})\Phi\vec{r}\right)^2 \tag{11}$$

$\delta_{\vec{k},\vec{k}_s} = 1$ if $\vec{k}_s = \vec{k}$, $\delta_{\vec{k},\vec{k}_s} = 0$ if $\vec{k}_s \neq \vec{k}$. To obtain equation (11) we used the $\vec{k}$-space representation of the Green function G_0 and separated variables of in-plane and normal-to-plane motion.

Note that in the oblique incidence case, equation (10) should be slightly modified. In particular, Θ_{nm} should be multiplied by in the TE polarization and divided by in the TM polarization, where α is the light propagation angle in the media. Moreover, in general, at oblique incidence, the exciton resonance is split into longitudinal, transverse and Z-polariton modes, which is neglected in our consideration since in realistic structures these effects are too fine to be observed.

We can further transform equation (10) bearing in mind that

$$\sum_{n=1}^{N}\Theta_{nm} \simeq \beta \cong \mathrm{i}\Gamma_r\int \mathrm{d}v\frac{f(v)}{v - \omega - \mathrm{i}\gamma} \qquad \Gamma_r = \frac{k}{2d^2}\omega_{LT}\pi a_B^3\left[\int \Phi(\vec{r})\cos(\vec{k}\vec{r})\,\mathrm{d}\vec{r}\right]^2 \tag{12}$$

where d is the average distance between two dots. Taking the exciton localization radius equal to the average radius r_{QD} of a QD, one can approximate the integral in formula (12) by r_{QD}/a_B^{2D} [16], where a_B^{2D} is the 2-dimensional exciton Bohr radius. The radiative broadening of the QW becomes

$$\Gamma_r = \frac{k}{2}\omega_{LT}\pi a_B^3\left(\frac{r_{QD}}{a_B^{2D}d}\right)^2. \tag{13}$$

We then obtain

$$\vec{E}_d(\omega,\vec{k}_s) = \vec{E}_0\delta_{\vec{k},\vec{k}_s} + \vec{E}_0\sum_{m=1}^{N}\frac{\mathrm{i}\Gamma_0^{QD}}{\omega_m - \omega - \mathrm{i}\gamma}\exp(\mathrm{i}\vec{k}_s\vec{R}_m)(1 - \beta)^{-1}. \tag{14}$$

Equation (14) is quite important for the following discussion, since it describes all kinds of coherent optical experiment (reflection, transmission and Rayleigh scattering) within the

same semi-classical formalism, properly taking into account the polariton effect. Γ_r is the radiative broadening of the exciton within the QW. It is proportional to the oscillator strength per unit area:

$$f = \frac{\sqrt{\varepsilon_b}}{\pi}\frac{mc}{e^2}\Gamma_r. \tag{15}$$

In the specular reflection direction, the formula (14) yields

$$r_{QW} = \frac{\beta}{1-\beta} \qquad t_{QW} = \frac{1}{1-\beta}. \tag{16}$$

Equation (16) is formally equivalent to the expressions for the reflection and transmission coefficients of a QW with an inhomogeneously broadened exciton resonance by Andreani *et al* [13] if one takes d and the in-plane size of a QD equal to the in-plane Bohr radius of a free exciton in a QW. We recover in that case $\Gamma_r = \Gamma_0$, the radiative broadening of the free exciton. The present formalism proves the validity of the phenomenological model [13] using a micro-model of a disordered array of QDs. Additionally, it allows us to calculate the amplitude of scattered light. The passage from the frequency-resolved to the time-resolved reflection and RRS spectra is simply achieved by the Fourier transform of equation (16).

In conclusion to this part, we have presented a unified semi-classical theory of propagation and scattering of exciton polaritons in heterostructures that has allowed us to describe time-resolved reflection and RRS spectra of QWs within the same formalism.

3. RRS measurements as a tool to characterize the QW excitons

Here we discuss the optical ways to characterize the spatial distribution of localized excitons in a QW, their energies and oscillator strengths. As before, attention will be paid mostly to the RRS experiments.

Consider that a laser pulse illuminates a single quantum well (SQW) under normal incidence at $t = 0$, and creates a coherent population of N excitons having a zero in-plane wavevector. These excitons in their turn coherently re-emit light in the reflected or transmitted directions within a lifetime $1/\Gamma_r$. They can also be coherently scattered within the time constant $1/\Delta$ and incoherently scattered within the time-constant $1/\gamma$. Within this description, the number $N_0(t)$ of excitons having a zero in-plane wave-vector at time t is

$$N_{k=0}(t) = N \exp\left(-\frac{\Delta^2 t^2}{2} - \Gamma_r t - \gamma t\right). \tag{17}$$

The integrated number of reflected photons N_{ref} is given by

$$N_{ref} = \int_0^\infty \Gamma_r N_{k=0}(t)\,\mathrm{d}t. \tag{18}$$

The integrated intensity of the reflected light is proportional to N_{ref}^2. In the nitride-based structures that are currently available, the condition $\Delta \gg \Gamma_0$ is fulfilled, that yields

$$I_{ref} = \frac{\pi}{2}N^2\frac{\Gamma_r^2}{\Delta^2}. \tag{19}$$

At the same time the total number of scattered excitons is given by

$$N_{k\neq 0} = \int_0^\infty \Delta N_{k=0}(t)\,\mathrm{d}t. \tag{20}$$

The intensity emitted in a single speckle is given by

$$I_{sca} = \frac{N_{k\neq 0}^2}{N} = \frac{\pi}{2}N. \tag{21}$$

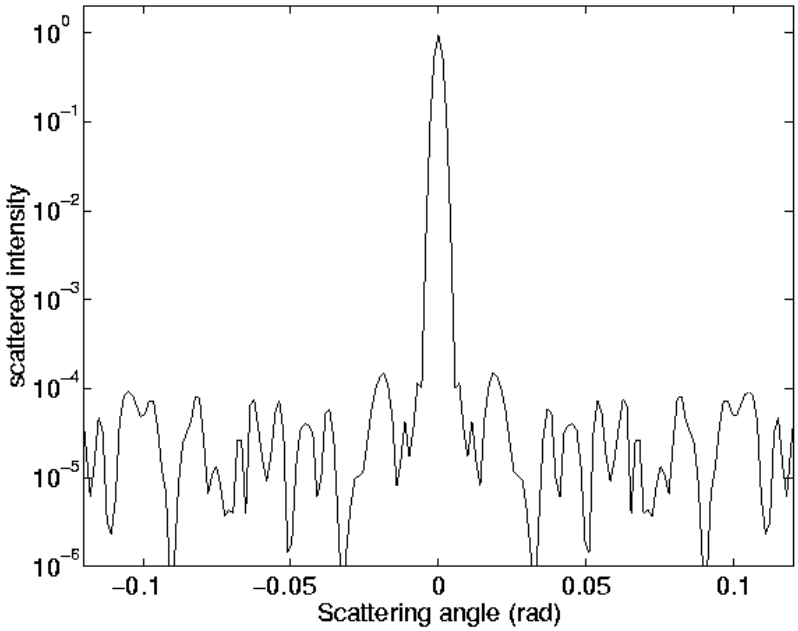

Figure 1. Integrated scattered intensity as a function of the scattering angle of a GaN/AlGaN single quantum well calculated with the formula (14). The parameters used are $N = 10^6$, $\Gamma_r = 0.5$ meV and $\Delta = 5$ meV and $n_b = \sqrt{\varepsilon_b} = 2.6$.

The ratio of the reflected intensity to the average scattered intensity is thus

$$I_{ref}/I_{scat} \approx N\left(\frac{\Gamma_r}{\Delta}\right)^2. \tag{22}$$

Figure 1 shows the integrated intensity as a function of the scattering angle calculated with the formula (14). The intensity for a scattering angle equal to zero corresponds to the reflected intensity. The average intensity obtained for the other angles is referred to as the scattered intensity. The calculation has been performed for $N = 10^6$, $\Gamma_r = 0.5$ meV and $\Delta = 5$ meV and for the background optical index $n_b = \sqrt{\varepsilon_b} = 2.6$. The ratio between reflection and scattering is 10^4 in perfect agreement with the estimation obtained from the formula (22).

As we will see in the third part of this article, one can extract the values of Γ_r and Δ from the cw reflectance spectra by a Fourier analysis. Once these two quantities are known, the number N of localized states within the light spot can be obtained using the formula (22), as well as the average distance between the dots.

It should be noted, however, that to obtain precise information on the statistics of excitons in a QW, the time-resolved RRS measurements are needed.

Typically a time-resolved RRS spectrum of an SQW exhibits a fast rise time $1/\Delta$ proportional to the scattering time of the exciton population created by the incident pulse followed by a decay time proportional at low temperature to $2/(\Gamma_r + \gamma)$. This means that the contributions of the inhomogeneous and of the radiative and homogeneous broadenings can be easily separated if one analyses the shape of the time-resolved RRS. Note also that γ is extremely small at low temperatures and can be easily obtained from independent photoluminescence measurements.

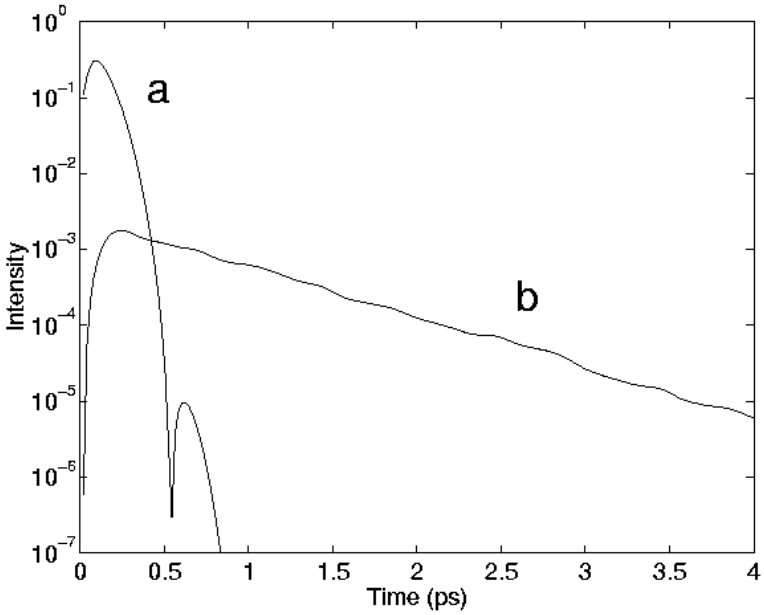

Figure 2. (a) Time-resolved reflection of a GaN/AlGaN single quantum well. (b) Time-resolved RRS of a GaN/AlGaN single quantum well. Both curves are obtained with the formula (14). The parameters used are $\Delta = 5$ meV, $\Gamma_r = 0.5$ meV, $\gamma = 0.001$ meV, $N = 10^6$. The diameter of the area excited by the incident laser pulse is taken to be 50 μm.

Figure 2 shows on the same scale the time-resolved reflection and the time-resolved RRS calculated with formula (14). The parameters are $\Delta = 5\,\text{meV}, \Gamma_r = 0.5\,\text{meV}, \gamma = 0.001\,\text{meV}$, $N = 10^6$. The diameter of the area excited by the incident laser pulse is taken to be 50 μm. From equations (22) and (14), the average ratio between the reflection speckle and a scattered speckle is 10^4. The reflection signal in figure 2 is obtained from a single speckle whereas the scattering signal is obtained from the averaging over 100 speckles. The ratio between the reflected and the scattered intensities is thus given by $10^4/100 = 10^2$ as one can see in figure 2. Note also the fast decay of the reflection that corresponds to the fast rise of the scattered signal. This latter becomes stronger than the reflection after only 500 fs, and then slowly decays with a characteristic time $2/\Gamma_r = 1.3$ ps.

Figure 3(a) shows the RRS of a single QW calculated for different values of Γ_r. We used the following set of parameters: $\Delta = 5$ meV, $\gamma = 0.001$ meV, $N = 10^6$. The values of Γ_r are 1 meV, 0.1 meV and 0.01 meV for the curves (a), (b) and (c), respectively. The advantage of this kind of experiment is here clearly seen. Indeed, it allows us to measure with a good accuracy the radiative broadening even if it is strongly dominated by the inhomogeneous broadening, that would be impossible in reflection. Figure 3(b) shows the RRS of a single QW calculated for different values of Δ. We always used $\Gamma_r = 0.5$ meV, $\gamma = 0.001$ meV, $N = 10^6$. The values of Δ are 20 meV, 2 meV and 0.2 meV for the curves (a), (b) and (c), respectively. Once again, the values of Δ and Γ_r can be easily obtained with the use of such a technique; the only limitation in case of large values of Δ comes from the time resolution of the experimental set-up.

4. Analysis of the reflection spectra of GaN/AlGaN QWs

In the previous papers [14, 15] we have presented the variational approach that allowed us to calculate the main excitonic parameters in GaN/AlGaN QWs taking into account the

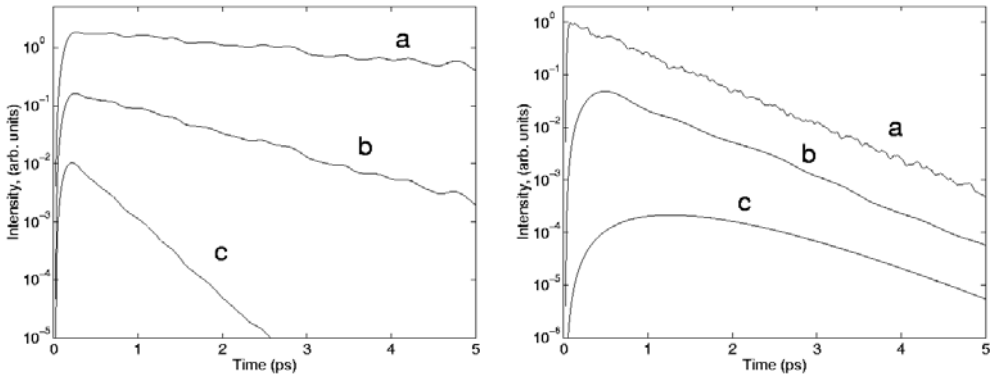

Figure 3. Left: time-resolved RRS of a single GaN/AlGaN QW calculated for different values of Γ_r. We used the following set of parameters: $\Delta = 5$ meV, $\gamma = 0.001$ meV, $N = 10^6$. The values of Γ_r are 1 meV, 0.3 meV and 0.1 meV for the curves (a), (b) and (c), respectively. Right: time-resolved RRS of a single GaN/AlGaN QW calculated for different values of Δ. We used the following set of parameters: $\Gamma_r = 0.5$ meV, $\gamma = 0.001$ meV, $N = 10^6$. The values of Δ are 20 meV, 2 meV and 0.2 meV for the curves (a), (b) and (c), respectively.

polarization fields and their eventual screening by a photoinduced free electron–hole plasma. To compare the results of these calculations with the experiment one has to find a way to extract the exciton oscillator strength from the available optical spectra.

This problem, that seems to be trivial at first glance, represents in fact a major difficulty for the optical characterization of nitrides. Actually, the exciton resonances in typical reflection or photoluminescence spectra of GaN-based QWs have a broadening of a few tens of meV. The origin of this broadening is in the potential disorder in-plane of the QWs that affects the excitons. This disorder is caused by the QW width fluctuations, alloy fluctuations and polarization field fluctuations. The excitonic spectrum is composed by contributions from millions of localized exciton states having different energies and oscillator strengths. In this situation the frequently used single-free-exciton-resonance model [3] fails to describe the real optical spectra.

This paper presents an alternative model, allowing us to analyse the exciton reflection spectra taking into account the exciton inhomogeneous broadening, and separating it numerically from the radiative broadening. This model has been applied to a series of reflection spectra taken by us from a series of high-quality MBE-grown GaN/$Al_{0.07}Ga_{0.93}N$ QW samples containing QWs of different thicknesses. The most essential conclusion of the performed analysis is that the oscillator strength in GaN/AlGaN QWs decreases with the QW width *much faster* than in conventional QWs. The collapse of the exciton oscillator strength in 10–12 monolayer-thick QWs is caused by distortion of excitons by the polarization fields, as our variational calculation confirms. Thus, only excitons in very thin QWs have the oscillator strength exceeding that in the bulk GaN.

Our method consists in the numerical Fourier transform of the experimental reflection spectrum of our sample and its comparison with the calculated time-resolved reflection coefficient, as illustrated by figure 4, that shows experimental and calculated frequency-resolved and time-resolved spectra of a 1 μm thick layer of GaN. A- and B-exciton resonances induce broad peaks of magnitude about 2%, while the background reflectivity is about 20%. In this case, the reflection coefficient of the structure can be written in the form

$$r(\omega) = r_0 + \Delta r(\omega) \tag{23}$$

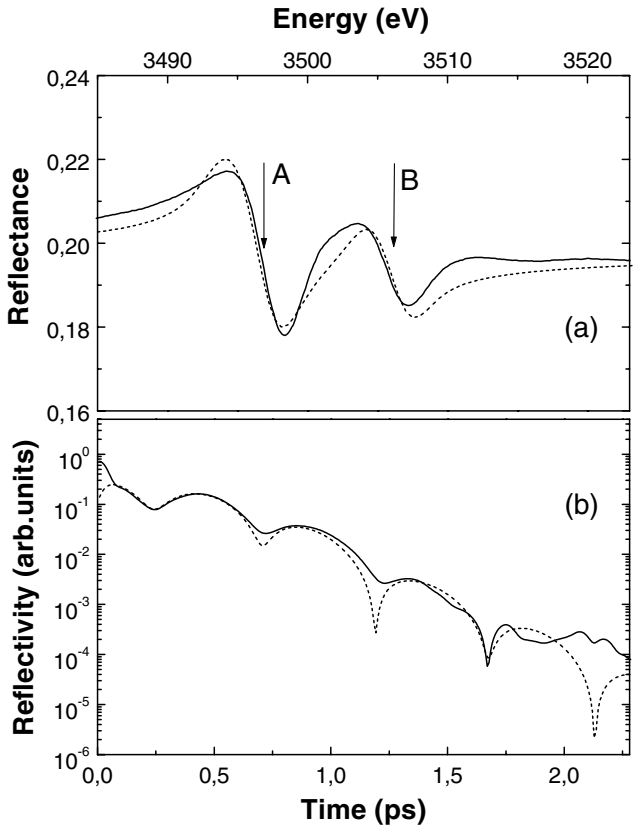

Figure 4. Frequency spectra (a) and time-resolved spectra (b) of a GaN layer grown on sapphire. Time-resolved reflectivity is determined by the Fourier transform of the experimental reflectance (solid lines); calculated reflectivity is shown by dashed lines.

where r_0 is the background coefficient, and the excitonic contribution can be expressed as

$$\Delta r(\omega) = \Delta a(\omega) + \mathrm{i}\Delta b(\omega)$$

with $\Delta a(\omega)$ being an odd real function and $\Delta b(\omega)$ being an even real function [9].

We convolute the measured reflectivity spectrum $|r(\omega)|^2$ with a broad Gaussian function $g(\omega)$ (that would correspond to a femtosecond incident light pulse in the case of a time-resolved measurement). For times longer than the pulse duration the Fourier transform of this quantity allows us to obtain

$$\int_{-\infty}^{+\infty} |g(\omega)r(\omega)|^2 \,\mathrm{e}^{-\mathrm{i}\omega t}\,\mathrm{d}\omega \cong 2r_0 \int_{-\infty}^{+\infty} g^2(\omega)\Delta a(\omega)\,\mathrm{e}^{-\mathrm{i}\omega t}\,\mathrm{d}\omega. \tag{24}$$

The approximate equality (24) is correct if Δa, $\Delta b \ll r_0$. The time-resolved reflection of a structure illuminated by a pulse $g^2(\omega)$ is

$$r_{g^2}(t) = \int_{-\infty}^{+\infty} g^2(\omega)r(\omega)\,\mathrm{e}^{-\mathrm{i}\omega t}\,\mathrm{d}\omega \cong 2\int_{-\infty}^{+\infty} g^2(\omega)\Delta a(\omega)\,\mathrm{e}^{-\mathrm{i}\omega t}\,\mathrm{d}\omega \tag{25}$$

that is proportional to the quantity given by equation (24). Thus, we have shown that for our experimental conditions, the numerical Fourier transform of the experimental reflectivity convoluted with a large spectral function yields formally the same spectrum (with a very high

accuracy) as the direct measurement of the time-resolved reflection by the femtosecond optical spectroscopy. The solid line in figure 4(b) represents the time-resolved reflection of the layer of bulk GaN obtained from the experimental spectrum shown in figure 4(a) as described above. It exhibits quite a rapid Gaussian-like decay typical for the systems with a strong exciton inhomogeneous broadening [16], and the pronounced oscillations that are nothing but beats between A- and B-exciton resonances.

The dashed curves in figure 4 are calculated using the generalized scattering state technique as described in [16]. We used the longitudinal transverse splittings for A and B excitons $\hbar\omega_{LT}^{A} = 1.7$ meV, $\hbar\omega_{LT}^{B} = 0.8$ meV, respectively, and their inhomogeneous broadenings of $\Delta_A = 2.2$ meV, $\Delta_B = 1.9$ meV. The difference between the two curves for extremely short times (<100 fs) comes from the finite pulse width we use (at the times comparable with the inverse pulse width, the approximate formula (25) is no longer valid). Otherwise, one can observe a fairly good agreement between theory and experiment, both in the cw and time-resolved spectra. The excitonic parameters are obtained with a quite good accuracy.

Once the technique allowing us to extract the excitonic characteristics from extremely broad spectral lines is established, we apply it to the series of $GaN/Al_{0.07}Ga_{0.93}N$ single QWs having different widths.

Figure 5(a) shows the measured (solid) and calculated (dashed) reflectivity of the $GaN/Al_{0.07}Ga_{0.93}N$ QW of 12 monolayer (ML) width. In figure 5(b) the solid line shows the time-resolved reflection obtained from the experimental reflectivity according to the formula (25) compared to the calculation with use of the semi-classical formalism [16] (dashed line). As for the bulk GaN sample, the fast decay of the time-resolved spectra is due to the high value of the inhomogeneous broadening. The inhomogeneous broadening has been assumed to be a Gaussian function characterized by a parameter Δ. The two other parameters of this model are the homogeneous broadening γ and the radiative broadening Γ_0 of the exciton line. At low temperature the value of the homogeneous broadening is negligible in comparison with Δ and Γ_0, thus only two parameters are to be determined. Δ characterizes the disorder within the QW and should decrease with the increase of the well thickness. Γ_0 characterizes the strength of exciton–light interaction and is proportional to the exciton oscillator strength [13]. The agreement between experiment and theory is quite good in figure 5. Once again, the difference at extremely short times comes from the limited accuracy of the transformation (3) in this time range. For times longer than 1.2 ps the experimental signal is dominated by noise and should not be taken into account. The comparison between experimental and theoretical curves allows us to extract Γ_0 and Δ (see figures 6(a) and (b)).

In order to observe the evolution of the radiative and inhomogeneous broadening as a function of the well thickness we have applied our procedure to a series of four high quality $GaN/Al_{0.07}Ga_{0.93}N$ QWs of 4, 8, 10 and 12 MLs. The results are summarized in figure 6, that shows the extracted points in comparison with theoretical curves calculated by the variational method [14, 15] for different concentrations of Al in the barriers. One can observe an extremely strong dependence of the radiative broadening on the thickness of the QW. The exciton oscillator strength decreases by a factor of 30 between 4 and 12 ML thick QWs, while the same variation of thickness of a GaAs/AlGaAs QW would cause the oscillator strength to decrease by only a factor of less than two [3]. This drastic dependence of the oscillator strength on the QW width is an important peculiarity of GaN/AlGaN QWs, that should be carefully taken into account when using these wells in light-emitting optical devices.

This dependence is mostly due to the strong polarization fields that are present in the nitride-based QWs. The fields spatially separate the electron and hole mass centres by a distance close to the well thickness. This considerably suppresses the overlap of electron

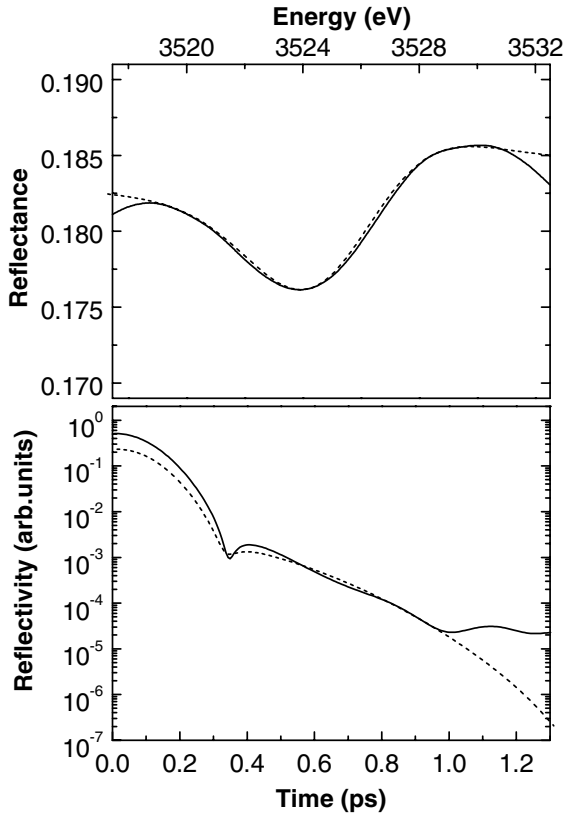

Figure 5. Frequency-resolved spectra (a) and time-resolved spectra (b) of an eight-monolayer-thick GaN–AlGaN QW.

and hole wave-functions leading to a collapse of the oscillator strength. This tendency has been predicted theoretically by variational calculations of the oscillator strength [14, 15]. We present here the first direct experimental evidence of this dependence.

The comparison of our data with the result of a variational calculation shows that the value of the polarization field in our QWs was about 700 kV cm^{-1}. Note that this value is sensitive to the aluminium concentration in the barriers and the barrier thickness. The value of 700 kV cm^{-1} seems on average to be the closest to the real value of the field, even if it is different in all the wells because of the different values of the strain and of the ratio of the well thickness over barrier thickness.

We would like to stress that despite the decrease of the exciton oscillator strength with the QW width, its absolute value is quite large in thin GaN/GaAlN QWs. So, the well of 8 ML width exhibits radiative broadening that is still one order of magnitude larger than in conventional GaAs or InGaAs QWs.

Figure 6(b) shows the evolution of the exciton inhomogeneous broadening Δ with the QW width. It is quite large compared to the typical GaAs-based structures and it strongly increases with decrease of the well thickness. However, it is worth noting that the ratio Γ_0/Δ is higher in the thin GaN/AlGaN wells than in most of the conventional III–V QWs (0.1 for the 8 ML well against 0.03 in a 10 nm thick GaAs/AlGaAs QW [3]). The high value of this ratio gives much hope for observation of the exciton-polariton propagation effects in the nitride-based

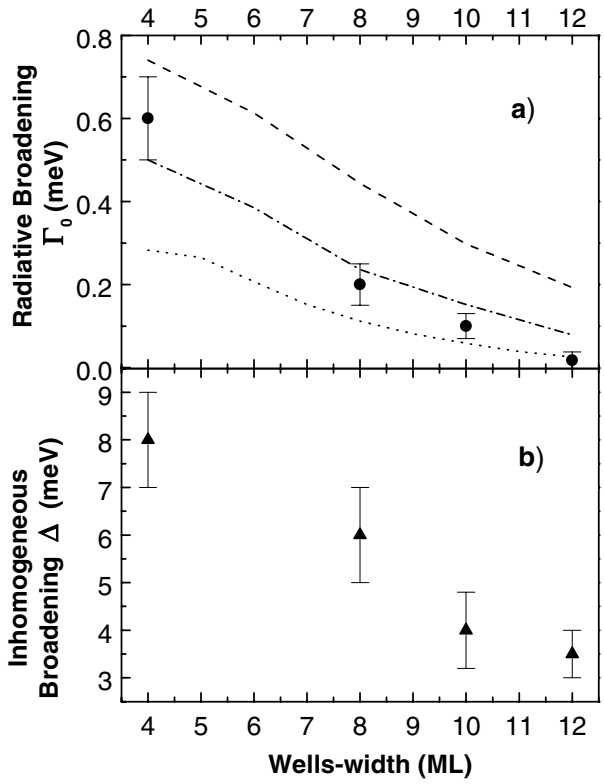

Figure 6. Well-width dependence of the oscillator strength Γ_0 (a) and inhomogeneous broadening Δ (b) of GaN–AlGaN QWs obtained from the spectra (solid circles) and calculated variationally (lines).

heterostructures [4, 7, 17, 18]. Let us note at this point that a multiple QW structure containing N wells would normally have the ratio of the radiative broadening to the inhomogeneous broadening equal to $N\Gamma_0/\Delta$. The coherent coupling of an exciton with light starts to dominate the disorder when this ratio becomes equal or superior to one, that we would expect to occur at $N > 10$. This proves, in particular, that the observation of the strong coupling regime [19] in nitride-based microcavities is a quite realistic task. This realization would open a way to the achievement of the stimulated scattering of microcavity polaritons [17, 18] at room temperature, which would represent a huge step forward in the realization of a new class of optoelectronic devices [20].

In conclusion, we have developed here a semi-classical theory of light–exciton coupling in strongly disordered GaN-based quantum structures. We have shown that the resonant Rayleigh scattering governs the coherent optical spectra of these structures, and that studying the RRS spectra one can obtain complex information on the exciton statistics, radiative and non-radiative broadening of exciton resonances, oscillator strength and localization radius. We have presented the first direct experimental study of the QW width effect on the radiative broadening and inhomogeneous broadening of excitons in $GaN/Al_{0.07}Ga_{0.93}N$ QWs. The major limitation of the accuracy of the experimental determination of these characteristics due to extremely broad exciton lines in the spectra has been eliminated by use of the original technique of numerical analysis of the spectra. The values of the radiative broadening we have

obtained are in a good agreement with the results of a variational calculation assuming the polarization field within the wells of 750 MV cm^{-1}. The collapse of the radiative broadening with the increase of the well width, and its high value for thin QWs, are evidenced. The significant value of the radiative broadening compared to the inhomogeneous broadening in thin GaN/AlGaN QWs makes them extremely promising for the observation of fine exciton-polariton effects. The stability of the excitons in nitrides at room temperature and their strong coupling with light give hope for realization of new classes of optoelectronic devices based on microcavity polaritons.

Acknowledgments

This work would have been impossible without numerous enlightening discussions with Bernard Gil who also provided us with all the optical spectroscopy data used in this paper. The samples were grown by N Grandjean and J Massies. We are indebted to M Zamfirescu and P Bigenwald for their numerical calculations used in this article. This work has been supported by the EU RTN 'CLERMONT' program, contract No HPRN-CT-1999-00132.

References

[1] Alemu A, Gil B, Julier M and Nakamura S 1998 *Phys. Rev.* B **57** 3761
[2] Hopfeld J J 1958 *Phys. Rev.* **112** 1555
Agranovich V M 1960 *Sov. Phys.–JETP* **37** 307
[3] For a review see Andreani L C 1995 *Confined Electrons and Photons* ed E Burstein and C Weisbuch (New York: Plenum) p 57
[4] Malpuech G, Kavokin A, Langbein W and Hvam J M 2000 *Phys. Rev. Lett.* **85** 650
[5] Langbein W, Hvam J M and Zimmermann R 1999 *Phys. Rev. Lett.* **82** 1040
[6] Malpuech G and Kavokin A 2001 *Phys. Status Solidi* a **183** 75
[7] Baumberg J J, Heberle A P, Kavokin A V, Vladimirova M R, and Köhler K 1998 *Phys. Rev. Lett.* **80** 3567
[8] EXAFS technique for example
[9] Malpuech G, Kavokin A, Leymarie J and Vasson A 2000 *Solid State Commun.* **113** 185
[10] Malpuech G, Kavokin A, Leymarie J, Disseix P and Vasson A 1999 *Phys. Rev.* B **60** 13 298
[11] Ivchenko E L and Kavokin A V 1992 *Sov. Phys.–Solid State* **34** 1815
[12] Malpuech G and Kavokin A 2001 *Semicond. Sci. Technol.* **16** R1
[13] Andreani L C, Panzarini G, Kavokin A V and Vladimirova M R 1998 *Phys. Rev.* B **57** 4670
[14] Bigenwald P, Kavokin A V, Gil B and Lefebvre P 2000 *Phys. Rev.* B **61** 15 621
[15] Bigenwald P, Kavokin A, Gil B and Lefebvre P 2001 *Phys. Rev.* B **63** 5315
[16] Kavokin A, Malpuech G and Panzarini G 1999 *Phys. Rev.* B **60** 788
[17] Huang R, Tassone F and Yamamoto Y 2000 *Phys. Rev.* B **61** R7854
Savvidis P G, Baumberg J J, Stevenson R M, Skolnick M, Whittaker D M and Roberts J S 2000 *Phys. Rev. Lett.* **84** 1547
[18] Stevenson R M, Astratov V N, Skolnick M S, Whittaker D M, Emam-Ismail M, Tartakovskii A I, Savvidis P G, Baumberg J J and Roberts J S 2000 *Phys. Rev. Lett.* **85** 3680
[19] Kavokin A and Gil B 1998 *Appl. Phys. Lett.* **72** 2880
[20] Yamamoto Y 2000 *Nature* **405** 629